

**Methane over  
South Asia**

X. Xiong et al.

# Methane plume over South Asia during the monsoon season: satellite observation and model simulation

X. Xiong<sup>1,2</sup>, S. Houweling<sup>3</sup>, J. Wei<sup>1,2</sup>, E. Maddy<sup>1,2</sup>, F. Sun<sup>1,2</sup>, and C. Barnet<sup>1</sup>

<sup>1</sup>NOAA/NESDIS/Center for Satellite Applications and Res., Camp Springs, Maryland, USA

<sup>2</sup>Perot Systems Government Services, Fairfax, Virginia, USA

<sup>3</sup>Netherlands Institute for Space Research, Utrecht, The Netherlands

Received: 18 April 2008 – Accepted: 10 June 2008 – Published: 15 July 2008

Correspondence to: X. Xiong (xiazhen.xiong@noaa.gov)

Published by Copernicus Publications on behalf of the European Geosciences Union.

Title Page

Abstract

Introduction

Conclusions

References

Tables

Figures

◀

▶

◀

▶

Back

Close

Full Screen / Esc

Printer-friendly Version

Interactive Discussion



## Abstract

Satellite observations of methane ( $\text{CH}_4$ ) using the Atmospheric Infrared Sounder (AIRS) on the EOS/Aqua platform from 2003–2007 demonstrate a strong, plume-like enhancement of  $\text{CH}_4$  in the middle to upper troposphere over the South Asia during July, August and September, and its maximum occurs in early September. Simulations using the global tracer model version 3 (TM3) also show similar seasonal enhancement of  $\text{CH}_4$  in the same region. The model results also suggest that this enhancement is associated with transport process and local surface emissions, thus the observations to tropospheric  $\text{CH}_4$  during the monsoon season may be used to constrain the models for a better estimation of Asian  $\text{CH}_4$  sources. Further comparisons between AIRS observations and the model simulations indicate a possible overestimate of  $\text{CH}_4$  emissions from rice paddies in Southeast Asia. Moreover, the observed tropospheric  $\text{CH}_4$  enhancement from AIRS provides evidence for the strong transport of atmospheric pollutants from the lower to the upper troposphere in Asia during the monsoon season, and the observed rapid disappearance of local  $\text{CH}_4$  maximum in September may provide valuable information for studying the dissipation of the Tibetan anticyclone and the withdrawal of monsoon.

## 1 Introduction

As the most important greenhouse gas next to carbon dioxide ( $\text{CO}_2$ ), methane ( $\text{CH}_4$ ) is about 20 times more powerful at warming the atmosphere than  $\text{CO}_2$  by weight, and plays an important role in atmospheric chemistry (IPCC, 2007). Therefore, understanding the emission sources of  $\text{CH}_4$  as well as its transport from surface to upper troposphere or even stratosphere is essential for climate change study. This problem is strikingly important over Southeast Asia as (a) the seasonal high emission of  $\text{CH}_4$  from rice paddies, a major  $\text{CH}_4$  emission source in this region (Khalil et al., 1998; Huang et al., 2004), and (b) the deep convection over the Tibetan Plateau (TP) occur

## Methane over South Asia

X. Xiong et al.

Title Page

Abstract

Introduction

Conclusions

References

Tables

Figures

◀

▶

◀

▶

Back

Close

Full Screen / Esc

Printer-friendly Version

Interactive Discussion



**Methane over  
South Asia**

X. Xiong et al.

[Title Page](#)[Abstract](#)[Introduction](#)[Conclusions](#)[References](#)[Tables](#)[Figures](#)[◀](#)[▶](#)[◀](#)[▶](#)[Back](#)[Close](#)[Full Screen / Esc](#)[Printer-friendly Version](#)[Interactive Discussion](#)

almost simultaneously in the same time during the monsoon season. By using satellite observation of carbon monoxide (CO) from Microwave Limb Sounder (MLS) and water vapor (H<sub>2</sub>O) from Tropical Rainfall-Measuring Missing satellite (TRMM), Fu et al. (2006) established that the TP provides the main pathway for cross-tropopause transport of water vapor and polluted air to the global stratosphere. Therefore, the transport of CH<sub>4</sub> from the Asia under the impact of the TP and the monsoon may constitute an important source pathway transporting CH<sub>4</sub> from lower to the upper atmosphere.

The Tibetan Plateau is located in the southwest of China and is the highest and biggest plateau in the world, with an area of 2.5 million km<sup>2</sup>. It is well known that the TP acts as a very strong heat source in summer and has a significant impact on the Asian Summer Monsoon (ASM). The intense convective activity generated at the TP and the large scale vertical motion associated with the ASM transport large amounts of sensible heat, moisture, chemical pollutants, as well as air with low ozone concentration from near-surface layers to upper layers (Ye and Wu, 1998 and references therein), as illustrated from many model simulations and observations. For example, model simulations (Lawrence et al., 2003; Liu et al., 2003) suggested that deep convection associated with the ASM lifts boundary layer pollutants from India, Southeast Asia, and southern China into the upper troposphere, and part of them can be transported westward by the tropical easterly jet to the Middle East (Li et al., 2001), and the Arabian sea (Filipiak et al., 2005), extensively influencing a part of Asia, Africa and Europe from June to September (Liu et al., 2003). Satellite observations have provided some evidences for the transport of atmospheric components from surface to the upper atmosphere. For example, the enhancements of CH<sub>4</sub>, water vapor and nitrogen oxides near the tropopause over the monsoon region were observed from Halogen Occultation Experiment (HALOE) measurement on Upper Atmosphere Research Satellite (UARS) (Park et al., 2004 and references therein); enhancement of CO was observed over India and southern China from Measurements Of Pollution In The Troposphere (MOPITT) (Kar et al., 2004) and over the TP and southwest China from EOS MLS (Li et al., 2005); and localized maximum of water vapor and minimum of ozone associated

with monsoon were observed from AIRS (Randel and Park, 2006).

In addition to the impact of large scale vertical motion associated with the ASM, the Tibetan anticyclone, which is one of the largest upper level anticyclones on Earth associated with the South Asia High (not always situated over Tibet), is another important component of understanding the structure of atmospheric components in the monsoon region (Li et al. 2005; Randel and Park, 2006). When the anthropogenic emissions from northeast India and southwest China were transported into the upper troposphere, they were entrained by the upper level Tibetan anticyclone (Li et al. 2005).

Previous satellite observations of CH<sub>4</sub> by HALOE were made only near and above the tropopause. Measurements by the Michelson Interferometer for Passive Atmospheric Sounding (MIPAS) on Envisat (Payan et al., 2007) and by the Atmospheric Chemistry Experiment (ACE) (Nassar et al., 2005; De Mazière et al., 2008) are in similar altitude region. Nadir-viewing measurement of tropospheric CH<sub>4</sub> has been made by the Interferometric Monitor for Greenhouse Gases (IMG) on board the Japanese Advanced Earth Observing Satellite (ADEOS) (Clerbaux et al., 2003) but only has a few months' data. So, up to now systematic measurements and analysis of the vertical variation of CH<sub>4</sub> in the middle to upper troposphere over the TP do not exist to our knowledge, and our knowledge about the distribution and transport of CH<sub>4</sub> in the monsoon region is poor, which is mainly attributed to the large uncertainty in the current estimation of CH<sub>4</sub> emissions from rice paddies in Asia (Huang et al., 2004; IPCC, 2007). Until recent observations by AIRS on EOS/Aqua, Xiong et al. (2008) have shown validated and valuable AIRS CH<sub>4</sub> products in the middle to upper troposphere for a couple years. As AIRS has the most sensitivity to CH<sub>4</sub> at 150–300 hPa near the tropics, which is just below the levels of the maximum confinement by Tibetan anticyclone at ~200–100 hPa (Randel and Park, 2006), the distribution of AIRS CH<sub>4</sub> in this altitude region could provide information on the Tibetan anticyclone. Therefore, analysis of AIRS CH<sub>4</sub> distribution can provide new insights into CH<sub>4</sub> emissions and transport in the monsoon region.

The aim of this paper is to explore the summer enhancement of CH<sub>4</sub> in south Asia us-

**Methane over South Asia**

X. Xiong et al.

Title Page

Abstract

Introduction

Conclusions

References

Tables

Figures

◀

▶

◀

▶

Back

Close

Full Screen / Esc

Printer-friendly Version

Interactive Discussion



**Methane over  
South Asia**

X. Xiong et al.

Title Page

Abstract

Introduction

Conclusions

References

Tables

Figures

◀

▶

◀

▶

Back

Close

Full Screen / Esc

Printer-friendly Version

Interactive Discussion



ing the data of CH<sub>4</sub> in the middle to upper troposphere from AIRS observation and the model simulation by an atmospheric transport model TM3 (Heimann and Körner, 2003; Houwelling et al., 2006). The seasonal variation of CH<sub>4</sub> in this region is studied in further detail by comparing AIRS observations with model simulations taking into account the averaging kernels characterizing AIRS retrieval skill (Maddy and Barnet, 2008). These comparisons demonstrate that the information of CH<sub>4</sub> observed from AIRS is reasonable. Moreover, an analysis of the seasonal change of AIRS CH<sub>4</sub> indicated that the observed tropospheric CH<sub>4</sub> enhancement and its disappearance provided some valuable information of the transport, including the dissipation of the Tibetan anticyclone and the withdrawal of monsoon.

To better understand the impact of dynamic transport on the formation of CH<sub>4</sub> plume, the monthly wind fields from National Oceanic and Atmospheric Administration (NOAA), National Centers for Environmental Prediction (NCEP) analysis data were analyzed. Furthermore, model simulations were carried out to investigate the sensitivity of CH<sub>4</sub> plume to the amount of the emission in Southeast Asia, and the results show that the enhancement of tropospheric CH<sub>4</sub> during the monsoon season is sensitive to surface emissions, suggesting the space-borne observations of tropospheric CH<sub>4</sub> in this period may provide a constraint to the models for the estimation of Asian CH<sub>4</sub> sources. Previous estimations of CH<sub>4</sub> emission sources and sinks from model were usually constrained using the ground-based measurement of tropospheric CH<sub>4</sub> concentration. From this perspective, AIRS CH<sub>4</sub> observation should be valuable for the study of global CH<sub>4</sub> sources and sinks.

## 2 Data and method

AIRS was launched in the polar orbit (01:30 p.m, ascending node) on National Aeronautics and Space Administration (NASA) EOS/Aqua platform in May 2002. It has 2378 channels covering from 649–1136, 1217–1613 and 2169–2674 cm<sup>-1</sup> at high spectral resolution ( $\lambda/\Delta\lambda=1200$ ,  $\sim 0.5$  cm<sup>-1</sup>) (Aumann et al., 2003), and the noise equivalent

**Methane over  
South Asia**

X. Xiong et al.

Title Page

Abstract

Introduction

Conclusions

References

Tables

Figures

◀

▶

◀

▶

Back

Close

Full Screen / Esc

Printer-friendly Version

Interactive Discussion



change in temperature ( $\text{NE}\Delta T$ ), at 250 K reference temperature, ranges from 0.14 K in the critical  $4.2\ \mu\text{m}$  lower tropospheric sounding wavelengths to 0.35 K in the  $15\ \mu\text{m}$  upper tropospheric sounding region. The spatial resolution of AIRS is 13.5 km at nadir, and in a 24-h period AIRS nominally observes the complete globe twice daily. In order to retrieve  $\text{CH}_4$  in both clear and partially cloudy scenes, 9 AIRS pixels in the footprint of an Advanced Microwave Sounding Unit (AMSU) pixel are used to derive the cloud-cleared radiance in this field of regard (FOR), from which the retrieval is made with the spatial resolution of about 45 km. The version 5 of AIRS product retrieval software (APS) has been put into operation at NASA Goddard Earth Sciences (GES) Data and Information Services Center (DISC), and these data are currently available at the Goddard DISC ([http://disc.gsfc.nasa.gov/AIRS/data\\_products.shtml](http://disc.gsfc.nasa.gov/AIRS/data_products.shtml)). An “off-line” version of the AIRS product has been run at Center for Satellite Application and Research, National Environmental Satellite, Data, and Information Service (NESDIS), NOAA to process AIRS data that is thinned in  $3\times 3$  degrees (latitude $\times$ longitude), and these data are used in this paper. As detailed by Xiong et al. (2008), over 70 AIRS channels near  $7.6\ \mu\text{m}$  are used for  $\text{CH}_4$  retrieval, and validation using in-situ aircraft observations showed the bias of the retrieved  $\text{CH}_4$  profiles is  $-1.4\sim+0.1\%$  and its rms difference is about  $0.5\text{--}1.6\%$  (Xiong et al., 2008). In general, the information content of AIRS observations near the tropics is larger than in other regions, so it is easier for AIRS to observe the variation of  $\text{CH}_4$  according to our validation using data in Hawaii and Rarotonga, Cook Islands ( $21.25^\circ\text{S}$ ,  $159.83^\circ\text{W}$ ). Due to the lack of in-situ observation over the TP, the validation to AIRS  $\text{CH}_4$  in the region studied in this paper can not be made. These uncertainties could hamper the accurate comparison of satellite data with model, but analysis of AIRS  $\text{CH}_4$  distribution and its seasonal change, and its comparison with model simulations allow us to make a qualitative assessment to the impact of transport and surface emissions during the monsoon season. To further reduce the uncertainty in the analysis of AIRS data, we tightened the quality control in addition to the quality control based on the degree of freedom as described by Xiong et al. (2008), and this was made by rejecting these profiles with obvious oscillation using a simple criterion

based on the variation range of CH<sub>4</sub> in the troposphere.

The global CH<sub>4</sub> concentration data from transport model simulations, as reported by Houweling et al. (2006), have been obtained using a source scenario (S3) as input to the atmospheric transport model TM3 (Heimann and Körner, 2003). This scenario, S3, includes direct plant emissions and the global emissions from rice is 60 Tgyr<sup>-1</sup> (see Table 1 in Houweling et al., 2006), but still has a little overestimate of CH<sub>4</sub> for South-east Asia in comparison with measurements from the surface and SCanning Imaging Absorption spectroMeter for Atmospheric CHartographY (SCIAMACHY) (Frankenberg et al., 2005). Model simulations have been performed on 3.75×5 degree horizontal resolution (latitude x longitude) for the period 2001–2004 with meteorological fields derived from the NCEP reanalysis (Kalnay et al., 1996). To test the sensitivity of the tropospheric CH<sub>4</sub> to surface emissions, we re-ran the model (denoted as the “2nd run”) by changing the surface emissions only. Since the uncertainty in the estimated CH<sub>4</sub> emissions from rice agriculture is large, for example, the estimated emissions can be from 31 to 112 Tgyr<sup>-1</sup> (IPCC, 2007 and references therein), for simplification, in the 2nd run we assumed an increase of CH<sub>4</sub> emissions by 50% in Southeast Asia in the region between 67.5° E–127.5° E and 3.83° N–42.13° N (denoted as region (I), the large box in the Fig. 1). The area with significant CH<sub>4</sub> enhancement considered in this paper is chosen in the region between 80° E–110° E and 20° N–35° N (denoted as region (II), the small box). The area of the region (I) is set to be much larger than the region (II) because the surface emissions from all area of the region (I) could possibly contribute to the formation of CH<sub>4</sub> plume in the region (II). The locations of regions (I) and (II) are evident in Fig. 1. The wind fields plotted in this paper are downloaded from NCEP/NOAA analysis data (<http://www.cdc.noaa.gov/cdc/data.ncep.reanalysis.html>).

Due to the change of information content inherent in the infrared observation, which is related to but not limited to the atmospheric temperature-moisture profiles, a good comparison of satellite observation with model simulation requires to use the averaging kernels to convolve the model data as below (Rodgers, 2000):

$$\hat{x} \approx Ax + (I - A)x_a \quad (1)$$

## Methane over South Asia

X. Xiong et al.

Title Page

Abstract

Introduction

Conclusions

References

Tables

Figures

◀

▶

◀

▶

Back

Close

Full Screen / Esc

Printer-friendly Version

Interactive Discussion



**Methane over  
South Asia**

X. Xiong et al.

[Title Page](#)[Abstract](#)[Introduction](#)[Conclusions](#)[References](#)[Tables](#)[Figures](#)[◀](#)[▶](#)[◀](#)[▶](#)[Back](#)[Close](#)[Full Screen / Esc](#)[Printer-friendly Version](#)[Interactive Discussion](#)

where  $\hat{x}$  is the convolved (or smoothed)  $\text{CH}_4$  mixing ratio profile,  $x$  is the profile from model simulations, and  $x_a$  is the first-guess profile (“a priori”), which is a function of latitude and pressure but does not vary with time and longitude (Xiong et al., 2008).  $\mathbf{I}$  is the identity matrix,  $A$  is the averaging kernels. In real application for AIRS,  $\log(x)$ ,  $\log(x_a)$ , and  $\log(\hat{x})$  are used in Eq. (1) (Maddy and Barnett, 2008). Differences between AIRS observations and the model convolved data will reflect the biases between satellite observation and the model simulation (as a “truth”) after taking into account the retrieval smoothing associated with the variation of information content in satellite observation. Unless otherwise stated, the model data in this paper have been convolved with AIRS averaging kernels.

### 3 Results and discussion

#### 3.1 Spatial distribution of tropospheric $\text{CH}_4$ over Southeast Asia from AIRS observations and model simulations

Significant increase of  $\text{CH}_4$  in the middle to upper troposphere was observed by AIRS in July, August and September, which is illustrated from the monthly mean distribution of  $\text{CH}_4$  at 300 hPa observed by AIRS and its counter part from model simulation (Fig. 1) in Southeast Asia. Model data are convolved using the corresponding monthly mean averaging kernels. The monthly horizontal wind fields at 300 hPa are overlaid with AIRS observations in the upper panels of Fig. 1, and the monthly horizontal winds at 150 hPa are plotted in the lower panels in order to demonstrate the strength and location of the Tibetan anticyclone. In July AIRS observed significant enhancement of  $\text{CH}_4$  over North India. In August both AIRS observation and model simulation show strong enhancement in the upper half of the the region (II). The maximum occurs in September with the area of significant  $\text{CH}_4$  enhancement extending slightly southward to lower part of the region (II). Overall, the location of the  $\text{CH}_4$  maximum as observed by AIRS is shifted westward compared with that of the model simulation. Particularly,

**Methane over  
South Asia**

X. Xiong et al.

in North India, higher  $\text{CH}_4$  is observed by AIRS than that from model simulation, while in Southeast China lower  $\text{CH}_4$  is observed by AIRS than that from model simulation. A recent study by Taniguchi and Koike (2008) indicates that there is more cloud activity over north Indian during June–July than middle May to June. Some similarity between the location of  $\text{CH}_4$  maximum with the location of Outgoing Longwave Radiation (OLR) (Fig. 13b in Taniguchi and Koike, 2008) indicates that uncertainties in the cloud-cleared radiances used in the AIRS  $\text{CH}_4$  retrieval algorithm may dominate the retrieved spatial structure over North India. The lower  $\text{CH}_4$  observed by AIRS than that from model simulation in the southeast China may be associated with the possible overestimate of  $\text{CH}_4$  emission in the model. However, we noticed that the  $\text{CH}_4$  maximum at 136 hPa observed by HALOE measurement is also toward the west of that from the simulations by the Model for Ozone and Related Chemical Tracers (MOZART) (Fig. 3 in Park et al., 2004). This consistency between HALOE (at a higher altitude) and AIRS observations may indicate some possible uncertainties exist in the models as well.

The formation of the  $\text{CH}_4$  plume is closely related with the circulation, which can be seen from the wind fields in Fig. 1. To better illustrate the relation of  $\text{CH}_4$  plume with circulation, we also compared the monthly change of  $\text{CH}_4$  mixing ratio at 300 hPa between AIRS observations and model simulation in Fig. 2. The monthly change is defined as  $\text{CH}_4$  mixing ratio in the present month divided by  $\text{CH}_4$  in the previous month, i.e.  $\text{CH}_4$  (present)/ $\text{CH}_4$  (previous)\*100.–100. The wind fields at 850 hPa from June to September are plotted in order to illustrate the dynamic transport in the lower troposphere. A careful examination to the wind fields at 850 hPa and 150 hPa shows that there is strong convergence around the TP (upper part of the region (II)) in July and August, and a strong anticyclone over the TP in August and September. The center of anticyclone moves southward slightly from around 30° N in August to 25° N in September. From June to July model simulations show that the most significant increase occurs in the center of the region (II), but AIRS observations show the area with significant increase is shifted northwestward in the region (II) and a larger enhancement westward of the region (II). Moreover, observations from AIRS suggest the transport is mainly from the

[Title Page](#)[Abstract](#)[Introduction](#)[Conclusions](#)[References](#)[Tables](#)[Figures](#)[I◀](#)[▶I](#)[◀](#)[▶](#)[Back](#)[Close](#)[Full Screen / Esc](#)[Printer-friendly Version](#)[Interactive Discussion](#)

**Methane over  
South Asia**

X. Xiong et al.

Middle East in the westerly jet, but this transport is relatively smaller in model simulation. Instead, model simulation shows a stronger transport northwestward across the Indian Subcontinent, which is likely associated with the propagation of the monsoon from June to early July. From July to August, the area with significant increase from model is more westward of that from AIRS. Model simulation also shows the transport is mainly from India as the monsoon moves to a higher altitude in the north of Indian Subcontinent, and the transport from northeast China along the northern branch of Tibetan anticyclone is relatively small. However, AIRS observation suggests that the strong convergence around the TP is the driver for the enhancement in the center of the region (II).

From August to September the area with significant increase from model is eastward of that from AIRS. Model simulation also shows the most significant increase of CH<sub>4</sub> occurs in Southeast of the TP, which is likely associated with the transport of CH<sub>4</sub> from southeast China along the southern slope of the TP in the easterly jet. But AIRS observation shows that the most significant enhancement occurs in northern India, and the impact of transport from southeast China is much smaller than that from model simulation. From the difference of the CH<sub>4</sub> in September and the CH<sub>4</sub> change from August to September between AIRS observation and model simulation, we suggest that the model possibly overestimates CH<sub>4</sub> emission from rice paddies in Southeast Asia, one of the main CH<sub>4</sub> emission sources in this period.

The uncertainties in AIRS retrievals include (a) the errors in atmospheric temperature and water moisture profiles, surface temperature and emissivity derived from other channels of AIRS over high terrain like the TP, particularly the increase of moisture imported by ASM to the TP region that pushes the most sensitive region of AIRS upward and makes the variation of the retrieved CH<sub>4</sub> confounded (Xiong et al., 2008), (b) the error in forward radiative transfer model (Strow et al., 2003), and (c) the error in cloud clearing that may be larger as more clouds have been observed to form over the TP region (Taniguchi and Koike, 2008). Therefore, instead of assessing whether AIRS observations to the CH<sub>4</sub> plume in Southeast Asia in the summer is better than model

[Title Page](#)[Abstract](#)[Introduction](#)[Conclusions](#)[References](#)[Tables](#)[Figures](#)[◀](#)[▶](#)[◀](#)[▶](#)[Back](#)[Close](#)[Full Screen / Esc](#)[Printer-friendly Version](#)[Interactive Discussion](#)

simulations, or vice versa, the aim of this comparison between AIRS observations and model simulations is to illustrate the existence of some difference between them, and call for more study in order to utilize AIRS observation in conjunction with model simulation to better quantify the Asian CH<sub>4</sub> sources and sinks in summer. Further validation to AIRS observation, as well as the improvement to AIRS retrieval algorithm and quality control will be the on-going efforts in the future.

### 3.2 Seasonal variation of CH<sub>4</sub> plume

Using the AIRS observations from August 2003 to December 2007, we computed their mean CH<sub>4</sub> profiles averaged in the region (II). To better illustrate the information content of AIRS retrieval and the retrieved seasonal variation of CH<sub>4</sub>, only the mean profiles from ascending node (daytime) during May to October 2004 are plotted in Fig. 3. Significant increase of CH<sub>4</sub> at 150–300 hPa is evident since early July and the maximum occurs at 5 September 2004. The most significant change of CH<sub>4</sub> occurs at pressure level between 150–300 hPa, reflecting the most sensitive regions of AIRS observations in these levels. In lower troposphere the sensitivity is small, so AIRS retrieved profiles tend to “stick to” the first guess and the seasonal variation can not be observed by AIRS.

Comparison of the seasonal variation of CH<sub>4</sub> in the region (II) from AIRS observations and model simulations was made after removing their mean from August 2003 to December 2007 separately (Fig. 4). This comparison of seasonal cycle instead of the absolute value of mixing ratio helps to reduce the bias between AIRS observation and model simulation. As the model data are not available 2005–2007, we used the data in 2004 instead, but convolved them using the averaging kernels corresponding to each AIRS observation. The seasonal change of about 100 ppb repeats every year, and the annual difference in the CH<sub>4</sub> maxima as well as its occurrence time are small. On average, the minimum of CH<sub>4</sub> occurs on 11 June and the maximum occurs on 7 September with a standard division of about 1 week. These dates of CH<sub>4</sub> plume occurrence and disappearance are closely related with the ASM, whose mean onset date is 4 June

## Methane over South Asia

X. Xiong et al.

Title Page

Abstract

Introduction

Conclusions

References

Tables

Figures

◀

▶

◀

▶

Back

Close

Full Screen / Esc

Printer-friendly Version

Interactive Discussion



**Methane over  
South Asia**

X. Xiong et al.

with a standard deviation of about 7.4 days and mean withdrawal date is 7 September with a standard deviation of about 11 days (Fasullo and Webster, 2003). CH<sub>4</sub> mixing ratio over south Asia decreases from its maximum quickly to the level in early June in about 10–12 days. The rapid decrease of CH<sub>4</sub> in September as compared to its slowly increase from June is also similar to the progress of monsoon that takes a longer time to develop but withdraws rapidly. Such a similarity of CH<sub>4</sub> variation with the onset and the withdrawal of ASM implies the important impact of dynamic transport associated with ASM on the formation of CH<sub>4</sub> plume, and the time for the disappearance of the CH<sub>4</sub> maximum observed from satellite may be used as an index to mark the withdrawal of the ASM.

As reported by Li et al. (2005), MLS and MOPITT observed the CO maximum during 25 August to 6 September 2004 over the TP and south China. This consistency of the CO and CH<sub>4</sub> maxima, as well as the local maximum of water vapor and the minimum of ozone, occurring at nearly the same time implies that the dynamic transport could be the most important factor driving the formation of the local maxima of water vapor, CH<sub>4</sub> and CO.

### 3.3 The pressure level dependence of the CH<sub>4</sub> enhancement and its relation with the anticyclone

By using the model simulation data, we computed the relative increase of CH<sub>4</sub> averaged in the region (II) from July to October as compared to the CH<sub>4</sub> mixing ratio in June. As shown in Fig. 5, the seasonal trend in different pressure levels is similar; however, the magnitude of the ratio of CH<sub>4</sub> in September to that in June, which we will assume to represent the “plume strength”, varies greatly with altitude. Below 300 hPa the plume strength increases with altitude, i.e. it increases from 2.7% at 600 hPa to 3.1% at 300 hPa. Above 300 hPa the plume strength decreases with altitude and it becomes 2.0% at 110 hPa. This transition of the variation of plume strength with altitude occurring at 110–200 hPa indicates the pressure levels where the Tibetan anticyclone locates. The existence of the Tibetan anticyclone at 110–200 hPa helps the

[Title Page](#)[Abstract](#)[Introduction](#)[Conclusions](#)[References](#)[Tables](#)[Figures](#)[◀](#)[▶](#)[◀](#)[▶](#)[Back](#)[Close](#)[Full Screen / Esc](#)[Printer-friendly Version](#)[Interactive Discussion](#)

**Methane over  
South Asia**

X. Xiong et al.

[Title Page](#)[Abstract](#)[Introduction](#)[Conclusions](#)[References](#)[Tables](#)[Figures](#)[I◀](#)[▶I](#)[◀](#)[▶](#)[Back](#)[Close](#)[Full Screen / Esc](#)[Printer-friendly Version](#)[Interactive Discussion](#)

accumulation of CH<sub>4</sub> and the formation of the CH<sub>4</sub> plume near 300 hPa, and in levels above the Tibetan anticyclone, i.e. 110 hPa, the seasonal increase of CH<sub>4</sub> mixing ratio from June to September is reduced significantly. In October, CH<sub>4</sub> mixing ratio decreases significantly in different levels with the most significant decrease occurring 200–300 hPa, indicating the rapid disappearance of the CH<sub>4</sub> plume in the middle to upper troposphere.

Consistent with model simulations, the significant increase of CH<sub>4</sub> in the middle to upper troposphere, as observed by AIRS, and the increase in the lower stratosphere, as observed by HALOE measurement (Park et al., 2004), provide evidences for the transport of CH<sub>4</sub> to the upper atmosphere. These observations suggest that this transport of CH<sub>4</sub> during the monsoon season may constitute an important source pathway by which CH<sub>4</sub> is transported from surface to stratosphere. Such a transport of CH<sub>4</sub> as well as the transport of water vapor and other trace gases to stratosphere during the monsoon season may play an important role in atmospheric chemistry, and is worthy of further study.

### 3.4 Sensitivity of CH<sub>4</sub> plume to CH<sub>4</sub> emissions from Southeast Asia

In order to investigate the relation between the enhancement of tropospheric CH<sub>4</sub> with the surface emissions, a sensitivity study was performed in which only the CH<sub>4</sub> emissions from Southeast Asia in the model were assumed to increase by 50% in the 2nd run. A comparison was made for the increase of CH<sub>4</sub> mixing ratio at 300 hPa from July to October as relative to the CH<sub>4</sub> mixing ratios of June corresponding to each run respectively. The results (Fig. 6) demonstrate that the relative enhancement of tropospheric CH<sub>4</sub> from June to September increases with the increase of surface emissions, so the larger the surface emission, the easier it is to detect the enhancement of tropospheric CH<sub>4</sub> in the middle to upper troposphere.

We also computed the difference of CH<sub>4</sub> mixing ratio at 300 hPa in these two runs. Here we used the CH<sub>4</sub> mixing ratio from the 2nd run divided by the CH<sub>4</sub> mixing ratio from the 1st run, i.e. CH<sub>4</sub> (2nd run)/CH<sub>4</sub> (1st run)\*100.-100., for each month from

**Methane over  
South Asia**

X. Xiong et al.

June to September (Fig. 7). This difference represents the relative change of  $\text{CH}_4$  corresponding to the increase of surface emissions. To account for the imbalance of  $\text{CH}_4$  sources and sinks in the 2nd run approximately, we subtracted the difference of background concentration of  $\text{CH}_4$  mixing ratio in the 2nd run from the 1st run, which is obtained as the mean mixing ratio over high southern hemispheric ocean. Significant increase of  $\text{CH}_4$  occurs in July, August and September with the maximum occurring in September. The locations of the largest increase of  $\text{CH}_4$  are also similar to the locations of the  $\text{CH}_4$  plume (Fig. 1). With a 50% increase of  $\text{CH}_4$  emissions in Southeast Asia, the monthly mean  $\text{CH}_4$  mixing ratio at 300 hPa over Southeast Asia increases up to 4–5% in September, which is overall significantly larger than the uncertainty in the AIRS retrieval. However, in reality the existence of the imbalance between the local sources and sinks in a limited time is possible, so the subtraction of the background difference of  $\text{CH}_4$  mixing ratio in these two runs may be inappropriate, and without subtracting this background difference, the monthly mean  $\text{CH}_4$  mixing ratio at 300 hPa over Southeast Asia increases up to 8–9% from June to September. Therefore, the observations of the  $\text{CH}_4$  plume over south Asia from space should be able to provide significant information of  $\text{CH}_4$  emissions in the summer.

#### 4 Summary and conclusions

Satellite observations of  $\text{CH}_4$  using AIRS on AQUA/EOS from August 2003 to December 2007 and some comparisons with model simulations using the TM3 were presented. They both showed similar enhancement of  $\text{CH}_4$  from June to September over South Asia. The maximum enhancement occurs in early September, and the value is up to 100 ppbv at 300 hPa from AIRS observations, and the increase of the monthly average from June to September is over 3% from model simulations. These results indicate that AIRS observations contain significant information about the transport of  $\text{CH}_4$  to the middle troposphere. The rapid disappearance of the  $\text{CH}_4$  plume observed by AIRS in September has a good correlation with the withdrawal of monsoon, sug-

[Title Page](#)[Abstract](#)[Introduction](#)[Conclusions](#)[References](#)[Tables](#)[Figures](#)[I◀](#)[▶I](#)[◀](#)[▶](#)[Back](#)[Close](#)[Full Screen / Esc](#)[Printer-friendly Version](#)[Interactive Discussion](#)

gesting this observation of CH<sub>4</sub> by AIRS may be valuable for studying the dissipation of the Tibetan anticyclone and the withdrawal of monsoon.

Consistent with other studies based on model simulations and/or observations, this observation of CH<sub>4</sub> enhancement in the middle to upper troposphere by AIRS provides additional evidence for the transport of chemical pollutants from the boundary layer to the upper troposphere over South Asia during the summer monsoon. While the deep convection and the Tibetan anticyclone are two important factors on the formation of local maximum of CH<sub>4</sub>, the seasonal high CH<sub>4</sub> emissions from rice paddies that occur almost simultaneously with the strong dynamic transport in the summer will result in a larger enhancement and transport of CH<sub>4</sub> than that of some other gases (like CO), which may constitute an important source pathway for CH<sub>4</sub> to be transported from the surface to the upper troposphere and stratosphere. The impact of this transport to the global CH<sub>4</sub> budget, particularly to the stratospheric CH<sub>4</sub>, should be worthy for more study.

Our model sensitivity study illustrated that surface source has played a major role in contributing to the mid to upper tropospheric enhancement of CH<sub>4</sub> in these regions influenced by the monsoon. For example, for an increase of CH<sub>4</sub> emissions from Southeast Asia by 50%, upper tropospheric CH<sub>4</sub> increases by up to 8–9% (or 4–5% if considering the imbalance of sources and sinks) over Southeast Asia in September. Therefore, observation to the CH<sub>4</sub> in the middle to upper troposphere and its seasonal change can provide valuable information of surface CH<sub>4</sub> sources in these regions in the summer. Such observation becomes possible by using of space-borne observations from AIRS and other operational thermal sounders, such as the Infrared Atmospheric Sounding Interferometer (IASI) on the METOP satellite series. Use of these data will enable us to better understand the CH<sub>4</sub> budget and study the global carbon cycle. However, more validation and improvement to AIRS/IASI retrieval of CH<sub>4</sub> need to be done before we can use their observation as a constraint of models to accurately estimate the Asian sources and sinks of CH<sub>4</sub>.

## Methane over South Asia

X. Xiong et al.

[Title Page](#)[Abstract](#)[Introduction](#)[Conclusions](#)[References](#)[Tables](#)[Figures](#)[I◀](#)[▶I](#)[◀](#)[▶](#)[Back](#)[Close](#)[Full Screen / Esc](#)[Printer-friendly Version](#)[Interactive Discussion](#)

*Acknowledgements.* This research was supported by funding from NOAA Office of Application & Research climate program. The views, opinions, and findings contained in this paper are those of the authors and should not be construed as an official National Oceanic and Atmospheric Administration or US Government position, policy, or decision.

## 5 References

Aumann, H. H., Chahine, M. T., Gautier, C., Goldberg, M. D., Kalnay, E., McMillin, L. M., Revercomb, H., Rosenkranz, P. W., Smith, W. L., Staelin, D. H., Strow, L. L., and Susskind, J.: AIRS/AMSU/HSB on the aqua mission: Design, science objectives, data products, and processing systems, *IEEE T. Geosci. Remote*, 41, 253–264, 2003.

10 Clerbaux, C., Hadji-Lazaro, J., Turquety, S., Mégie, G., and Coheur, P.-F.: Trace gas measurements from infrared satellite for chemistry and climate applications, *Atmos. Chem. Phys.*, 3, 1495–1508, 2003,  
<http://www.atmos-chem-phys.net/3/1495/2003/>.

15 De Mazière, M., Vigouroux, C., Bernath, P. F., Baron, P., Blumenstock, T., Boone, C., Brogniez, C., Catoire, V., Coffey, M., Duchatelet, P., Griffith, D., Hannigan, J., Kasai, Y., Kramer, I., Jones, N., Mahieu, E., Manney, G. L., Piccolo, C., Randall, C., Robert, C., Senten, C., Strong, K., Taylor, J., Tétard, C., Walker, K. A., and Wood, S.: Validation of ACE-FTS v2.2 methane profiles from the upper troposphere to the lower mesosphere, *Atmos. Chem. Phys.*, 8, 2421–2435, 2008,  
<http://www.atmos-chem-phys.net/8/2421/2008/>.

20 Fasullo, J. and Webster, P. J.: A hydrological definition of indian monsoon onset and withdrawal, *J. Climate*, 16, 3200–3211, 2003.

25 Filipiak, M. J., Harwood, R. S., Jiang, J. H., Li, Q. B., Livesey, N. J., Manney, G. L., Read, W. G., Schwartz, M. J., Waters, J. W., and Wu, D. L.: Carbon monoxide measured by the EOS microwave limb sounder on Aura: First results, *Geophys. Res. Lett.*, 32, L14825, doi:10.1029/2005GL02276, 2005.

Frankenberg, C., Meirink, J. F., van Weele, M., Platt, U., and Wagner, T.: Assessing methane emissions from global space-borne observations, *Science*, 308, 1010–1014, 2005.

30 Fu, R., Hu, Y., Wright, J. S., Jiang, J. H., Dickinson, R. E., Chen, M., Filipiak, M., Read, W. G., Waters, J. W., and Wu, D. L.: Short circuit of water vapor and polluted air to the global

## Methane over South Asia

X. Xiong et al.

Title Page

Abstract

Introduction

Conclusions

References

Tables

Figures

◀

▶

◀

▶

Back

Close

Full Screen / Esc

Printer-friendly Version

Interactive Discussion



**Methane over  
South Asia**

X. Xiong et al.

Title Page

Abstract

Introduction

Conclusions

References

Tables

Figures

◀

▶

◀

▶

Back

Close

Full Screen / Esc

Printer-friendly Version

Interactive Discussion



stratosphere by convective transport over the Tibetan Plateau, Proceedings of the National Academy of Sciences (PNAS), 103, 5664–5669, 2006.

Heimann, M. and Körner, S.: The global atmospheric tracer model TM3, Max Planck Institute of Biogeochemistry, Model description and user's manual, Release 3.8a, 2003.

5 Houweling, S., Rockmann, T., Aben, I., Keppler, F., Krol, M., Meirink, J. F., Dlugokencky, E. J., and Frankenberg, C.: Atmospheric constraints on global emissions of methane from plants, Geophys. Res. Lett., 33, L15821, doi:10.1029/2006GL026162, 2006.

Huang, Y., Zhang, W., Zheng, X. H., Li, J., and Yu, Y. Q.: Modeling methane emission from rice paddies with various agricultural practices, J. Geophys. Res.-Atmos., 109, D08113, doi:10.1029/2003JD004401, 2004.

10 Intergovernmental Panel on Climate Change: Climate Change 2007: The Physical Science Basis, Contribution of Working Group I to the Fourth Assessment Report of the Intergovernmental Panel on Climate Change, edited by: Solomon, S., Qin, D., Manning, M., Chen, Z., Marquis, M., Averyt, K. B., Tignor, M., and Miller, H. L., Cambridge University Press, Cambridge, United Kingdom and New York, NY, USA, 500–590, 2007.

15 Kalnay, E., Kanamitsu, M., Kistler, R., Collins, W., Deaven, D., Gandin, L., Iredell, M., Saha, S., White, G., Woollen, J., Zhu, Y., Chelliah, M., Ebisuzaki, W., Higgins, W., Janowiak, J., Mo, K. C., Ropelewski, C., Wang, J., Leetmaa, A., Reynolds, R., Jenne, R., and Joseph, D.: The NCEP/NCAR 40-year reanalysis project, B. Am. Meteorol. Soc., 77, 437–471, 1996.

20 Kar, J., Bremer, H., Drummond, J. R., Rochon, Y. J., Jones, D. B. A., Nichitiu, F., Zou, J., Liu, J., Gille, J. C., Edwards, D. P., Deeter, M. N., Francis, G., Ziskin, D., and Warner, J.: Evidence of vertical transport of carbon monoxide from measurements of pollution in the troposphere (MOPITT), Geophys. Res. Lett., 31, L23105, doi:10.1029/2004GL021128, 2004.

25 Khalil, M. A. K., Rasmussen, R. A., Shearer, M. J., Dalluge, R. W., Ren, L. X., and Duan, C. L.: Measurements of methane emissions from rice fields in China, J. Geophys. Res.-Atmos., 103, 25 181–25 210, 1998.

Lawrence, M. G., Rasch, P. J., von Kuhlmann, R., Williams, J., Fischer, H., de Reus, M., Lelieveld, J., Crutzen, P. J., Schultz, M., Stier, P., Huntrieser, H., Heland, J., Stohl, A., Forster, C., Elbern, H., Jakobs, H., and Dickerson, R. R.: Global chemical weather forecasts for field campaign planning: Predictions and observations of large-scale features during minos, contrace, and indoex, Atmos. Chem. Phys., 3, 267–289, 2003,

<http://www.atmos-chem-phys.net/3/267/2003/>.

30 Li, Q. B., Jacob, D. J., Logan, J. A., Bey, I., Yantosca, R. M., Liu, H. Y., Martin, R. V., Fiore, A.

**Methane over  
South Asia**

X. Xiong et al.

M., Field, B. D., Duncan, B. N., and Thouret, V.: A tropospheric ozone maximum over the middle east, *Geophys. Res. Lett.*, 28, 3235–3238, 2001.

Li, Q. B., Jiang, J. H., Wu, D. L., Read, W. G., Livesey, N. J., Waters, J. W., Zhang, Y. S., Wang, B., Filipiak, M. J., Davis, C. P., Turquety, S., Wu, S. L., Park, R. J., Yantosca, R. M., and Jacob, D. J.: Convective outflow of south asian pollution: A global ctm simulation compared with EOS MLS observations, *Geophys. Res. Lett.*, 32, L14826, doi:10.1029/2005GL022762, 2005.

Liu, Y., Li, W. L., Zhou, X. J., Isaksen, I. S. A., Sundet, J. K., and He, J. H.: The possible influences of the increasing anthropogenic emissions in India on tropospheric ozone and OH, *Adv. Atmos. Sci.*, 20, 968–977, 2003.

Maddy, E. S. and Barnet, C. D.: Vertical resolution estimates in Version 5 of AIRS operational retrievals, *IEEE T. Geosci. Remote*, 46, 8, 2008.

Nassar, R., Bernath, P. F., Boone, C. D., Manney, G. L., McLeod, S. D., Rinsland, C. P., Skelton, R., and Walker, K. A.: Stratospheric abundances of water and methane based on ACE-FTS measurements, *Geophys. Res. Lett.*, 32, L15S04, doi:10.1029/2005GL022383, 2005.

Payan, S., Camy-Peyret, C., Oelhaf, H., Wetzell, G., Maucher, G., Keim, C., Pirre, M., Huret, N., Engel, A., Volk, M. C., Kuehlmann, H., Kuttippurath, J., Cortesi, U., Bianchini, G., Men-caraglia, F., Raspollini, P., Redaelli, G., Vigouroux, C., De Mazière, M., Mikuteit, S., Blumenstock, T., Velazco, V., Notholt, J., Mahieu, M., Duchatelet, P., Smale, D., Wood, S., Jones, N., Piccolo, C., Payne, V., Bracher, A., Glatthor, N., Stiller, G., Grunow, K., Jeseck, P., Te, Y., Pfeilsticker, K., and Butz, A.: Validation and data characteristics of methane and nitrous oxide profiles observed by MIPAS and processed with Version 4.61 algorithm, *Atmos. Chem. Phys. Discuss.*, 7, 18 043–18 111, 2007.

Park, M., Randel, W. J., Kinnison, D. E., Garcia, R. R., and Choi, W.: Seasonal variation of methane, water vapor, and nitrogen oxides near the tropopause: Satellite observations and model simulations, *J. Geophys. Res.-Atmos.*, 109, D03302, doi:10.1029/2003JD003706, 2004.

Randel, W. J. and Park, M.: Deep convective influence on the asian summer monsoon anticyclone and associated tracer variability observed with atmospheric infrared sounder (AIRS), *J. Geophys. Res.-Atmos.*, 111, D12314, doi:10.1029/2005JD006490., 2006.

Rodgers, C. D.: *Inverse Methods for Atmospheric Sounding*, World Sci., Hackensack, N. J., 2000.

Strow, L. L., Hannon, S. E., De Souza-Machado, S., Motteler, H. E., and Tobin, D.: An overview

[Title Page](#)[Abstract](#)[Introduction](#)[Conclusions](#)[References](#)[Tables](#)[Figures](#)[◀](#)[▶](#)[◀](#)[▶](#)[Back](#)[Close](#)[Full Screen / Esc](#)[Printer-friendly Version](#)[Interactive Discussion](#)

of the airs radiative transfer model, IEEE T. Geosci. Remote, 41, 303–313, 2003.

Taniguchi, K. and Koike, T.: Seasonal Variation of Cloud Activity and Atmospheric Profiles over the Eastern Part of the Tibetan Plateau, J. Geophys. Res., 113, D10104, doi:10.1029/2007JD009321, 2008

5 Xiong, X., Barnet, C. D., Maddy, E. , Sweeney, C. , Liu, X. , Zhou, L., and Goldberg, M.: Characterization and Validation of Methane Products from the Atmospheric Infrared Sounder (AIRS), J. Geophys. Res., 113, G00A01, doi:10.1029/2007JG000500, 2008.

Ye, D. Z. and Wu, G. X.: The role of the heat source of the tibetan plateau in the general circulation, Meteorol. Atmos. Phys., 67, 181–198, 1998.

10

ACPD

8, 13453–13478, 2008

---

## Methane over South Asia

X. Xiong et al.

---

Title Page

Abstract

Introduction

Conclusions

References

Tables

Figures

◀

▶

◀

▶

Back

Close

Full Screen / Esc

Printer-friendly Version

Interactive Discussion



Methane over  
South Asia

X. Xiong et al.

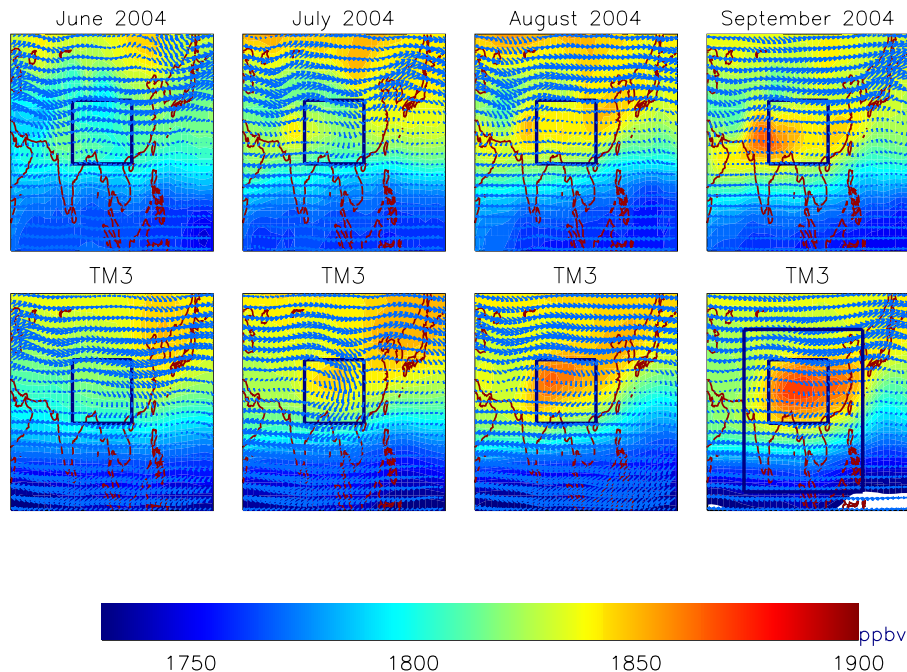


**Fig. 1.** Spatial variation of monthly mean  $\text{CH}_4$  at 300 hPa from June to September 2004 in Southeast Asia observed from AIRS observation (top) and model simulation using the TM3 (bottom). Significant enhancement of  $\text{CH}_4$  is evident in August and September. The wind fields at 300 hPa (top) and 150 hPa (bottom) are shown respectively.

[Title Page](#)[Abstract](#)[Introduction](#)[Conclusions](#)[References](#)[Tables](#)[Figures](#)[I◀](#)[▶I](#)[◀](#)[▶](#)[Back](#)[Close](#)[Full Screen / Esc](#)[Printer-friendly Version](#)[Interactive Discussion](#)

Methane over  
South Asia

X. Xiong et al.

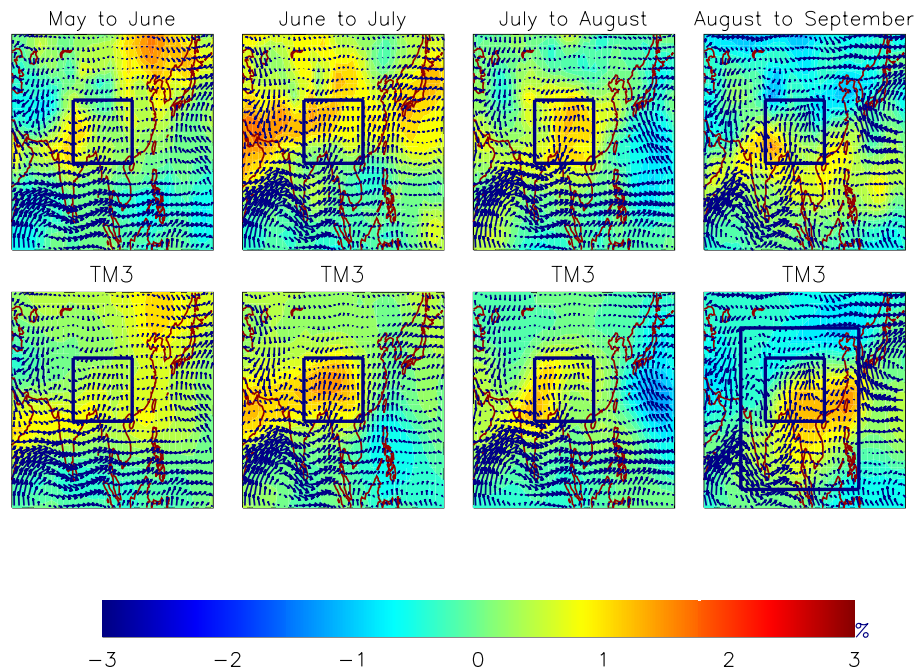


**Fig. 2.** Spatial variation of the monthly changed  $\text{CH}_4$  at 300 hPa observed by AIRS (top) and model simulation (bottom). The wind fields at 850 hPa are shown.

[Title Page](#)[Abstract](#)[Introduction](#)[Conclusions](#)[References](#)[Tables](#)[Figures](#)[◀](#)[▶](#)[◀](#)[▶](#)[Back](#)[Close](#)[Full Screen / Esc](#)[Printer-friendly Version](#)[Interactive Discussion](#)

**Methane over  
South Asia**

X. Xiong et al.

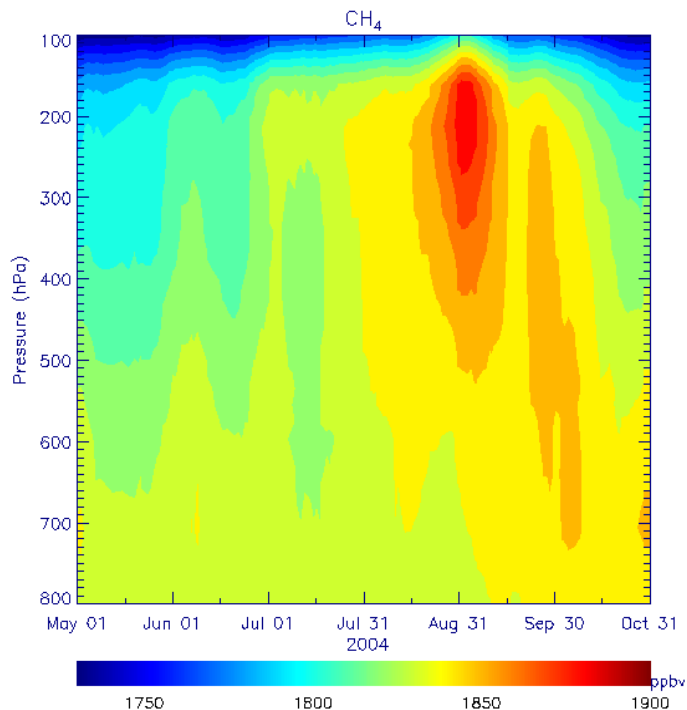


**Fig. 3.** Time-pressure cross section of AIRS CH<sub>4</sub> averaged in the region (II). Data is from ascending node (01:30 p.m. LST). Significant enhancement of CH<sub>4</sub> at middle to upper troposphere is evident with the maximum occurring in early September.

[Title Page](#)[Abstract](#)[Introduction](#)[Conclusions](#)[References](#)[Tables](#)[Figures](#)[◀](#)[▶](#)[◀](#)[▶](#)[Back](#)[Close](#)[Full Screen / Esc](#)[Printer-friendly Version](#)[Interactive Discussion](#)

**Methane over  
South Asia**

X. Xiong et al.

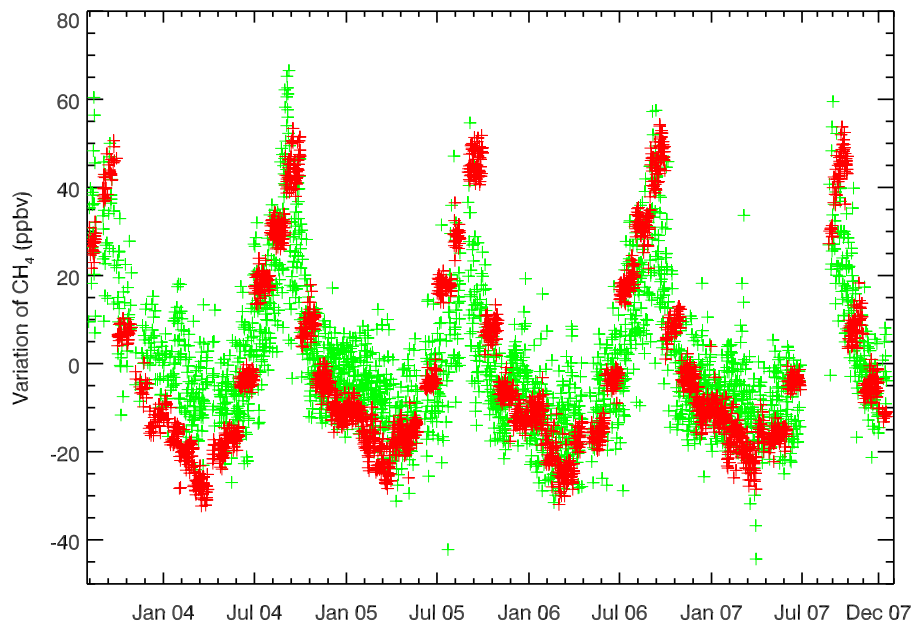


**Fig. 4.** Seasonal variation of  $\text{CH}_4$  at 300 hPa averaged in the region (II) from August 2003 to December 2007. Blue is AIRS observations. Red is the model data in 2004 convolved with averaging kernels from every AIRS observation. The  $\text{CH}_4$  increase from June to September is up to 100 ppbv with small annual difference.

[Title Page](#)[Abstract](#)[Introduction](#)[Conclusions](#)[References](#)[Tables](#)[Figures](#)[I◀](#)[▶I](#)[◀](#)[▶](#)[Back](#)[Close](#)[Full Screen / Esc](#)[Printer-friendly Version](#)[Interactive Discussion](#)

**Methane over  
South Asia**

X. Xiong et al.

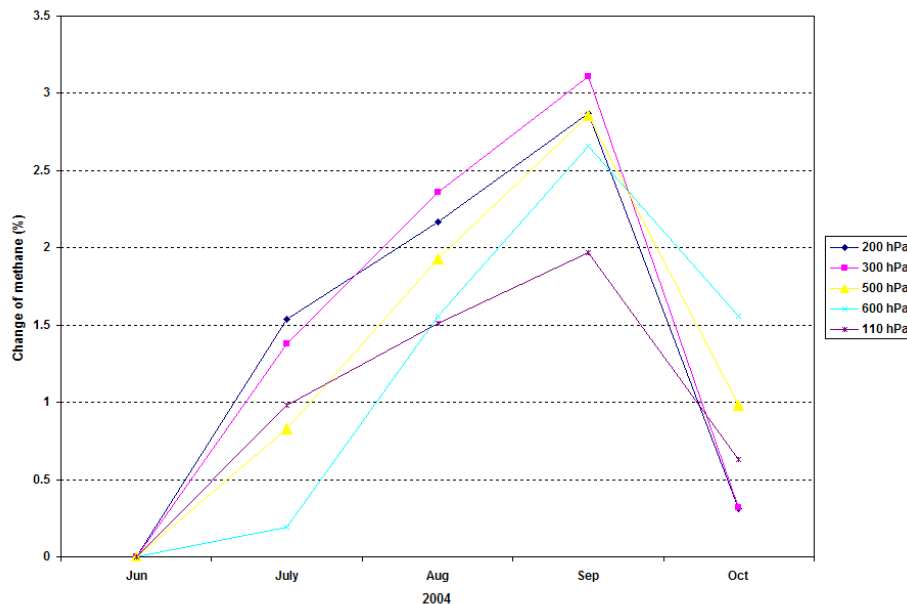


**Fig. 5.** Seasonal change of CH<sub>4</sub> averaged in the region (II) from July to October (relative to June) and its dependence with pressure levels. All data are from model simulation only.

[Title Page](#)[Abstract](#)[Introduction](#)[Conclusions](#)[References](#)[Tables](#)[Figures](#)[I◀](#)[▶I](#)[◀](#)[▶](#)[Back](#)[Close](#)[Full Screen / Esc](#)[Printer-friendly Version](#)[Interactive Discussion](#)

**Methane over  
South Asia**

X. Xiong et al.

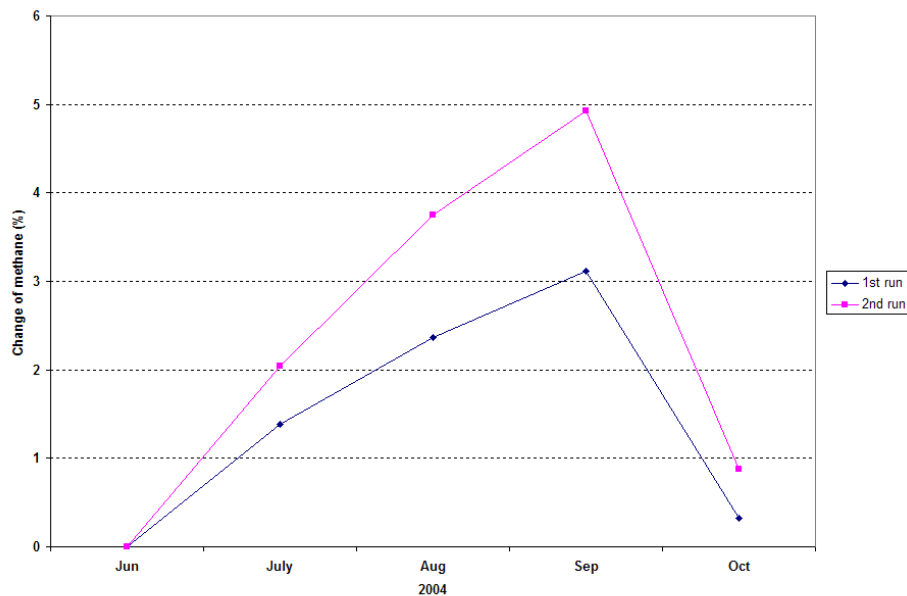


**Fig. 6.** Seasonal change of  $\text{CH}_4$  averaged in the region (II) from July to October (relative to June) for two different runs. The only difference between them is that in the 2nd run the  $\text{CH}_4$  emissions in Southeast Asia is increased by 50% than that in the 1st run. All data are from model simulation only.

[Title Page](#)[Abstract](#)[Introduction](#)[Conclusions](#)[References](#)[Tables](#)[Figures](#)[I◀](#)[▶I](#)[◀](#)[▶](#)[Back](#)[Close](#)[Full Screen / Esc](#)[Printer-friendly Version](#)[Interactive Discussion](#)

Methane over  
South Asia

X. Xiong et al.

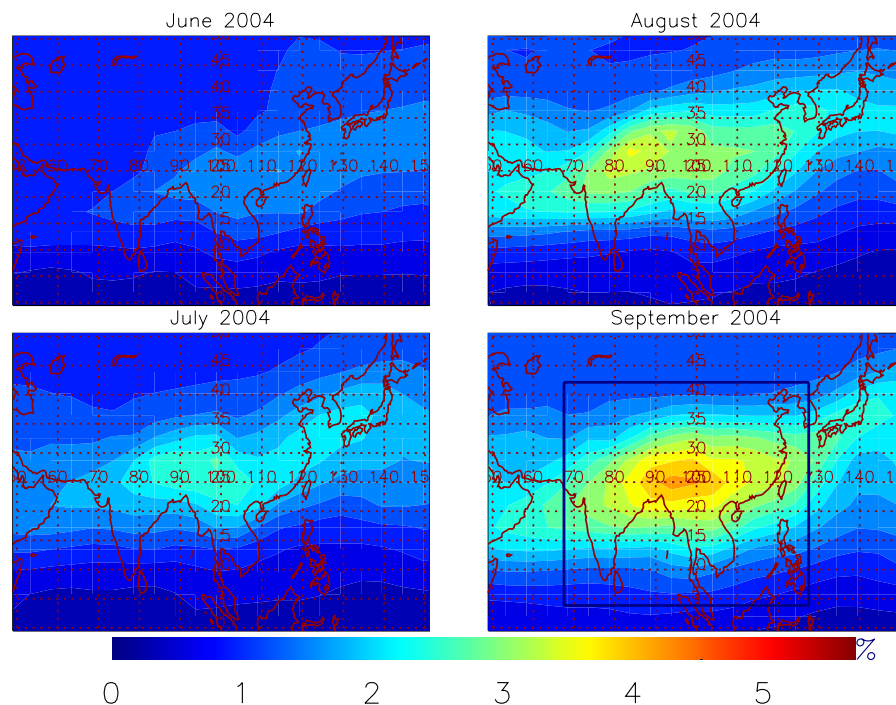


**Fig. 7.** Spatial distribution of the relative increase of CH<sub>4</sub> mixing ratio at 300 hPa corresponding to 50% increase of CH<sub>4</sub> emissions over Southeast Asia (region (I), as marked in the box). The change of background concentration has been removed to account for the imbalance between the sources and sinks after 50% increase of CH<sub>4</sub> emissions. All data are from model simulation only.

[Title Page](#)[Abstract](#)[Introduction](#)[Conclusions](#)[References](#)[Tables](#)[Figures](#)[◀](#)[▶](#)[◀](#)[▶](#)[Back](#)[Close](#)[Full Screen / Esc](#)[Printer-friendly Version](#)[Interactive Discussion](#)